Numerical simulation of initial perturbation growth in oblique impact of metal plates

Bakhrakh S.M., Volodina N.A., Nizovtsev P.N., Spiridonov V.F., Shuvalova E.V.
VNIIEF-RUSSIA

Introduction

An oblique impact of metal layers results in development of intensive shear strains at their interface, the near-boundary metal layers become severely heated and produce shaped jets. These effects lead to the interface profile distortion. Both regular and asymmetric distorted waves appear. In this case a hydrodynamic instability, the Kelvin-Helmholtz instability, appears [1].

The subsonic regime of the oblique impact has been comprehensively studied recently, where $U_c<C_s$ (U_c – contact point velocity, C_s – sound speed in the material). Under these loading conditions, a shaped jet forms at the contact point, if the pressure about the impact point is higher than the metal strength.

The initial perturbation growth is known to occur in the subsonic impact conditions in the gas dynamics approximation. The situation is more complex in the supersonic impact of strong plates.

When the impact angle is constant, there is critical velocity U_{cr}. If $C_s<U_c<U_{cr}$, detached oblique shock waves form in the flow. During the transition across the wave front the flow transforms from supersonic to subsonic. In the impact zone the shaped jet forms and the perturbations grow like in the case of the subsonic impact.

When $U_c> U_{cr}$, attached oblique shock waves are established at the contact point and no jet formation is observed. The perturbation evolution is considered as impossible in this case, as there is no principal perturbation generator, i.e. the shaped jet.

The material interface state in such supersonic loading conditions has been inadequately studied. It was anticipated that essentially prompt cessation of the perturbation evolution process would be obtained in the transition to the jet-free conditions of the plate impact. That is, as soon as $U_c= U_{cr}$, no peturbations should appear. However, the perturbation growth was observed in the experiments. Ref. [2] analyzes the experimental data and explains this phenomenon theoretically.

The direct numerical simulation of the experiments is of interest.

1. Numerical codes. Setting up problems

The numerical simulations were performed with the program complex that implements code LEGAK [3].

The strength properties are included using code [4].

The material state was described in the elastic-plastic approximation. Pressure was estimated by Mie-Grueneisen equation of state [5] with the following parameters:

$$\rho_0 = 2.64\frac{g}{cm^3},\ c_0 = 5.55\frac{km}{s},\ \boldsymbol{n = 3.2},\ \boldsymbol{\Gamma = 2.14}.$$

Yield strength was taken as a function of pressure and temperature:

$$\boldsymbol{Y = Y_0 (1 + \alpha \cdot P)\left(1 - \beta \cdot \frac{E_T}{E_m}\right)},$$

where $\boldsymbol{Y_0 = 0.3}$, $\alpha = \frac{1}{3}$, $\beta = 1$, E_T is heat energy, $E_m = 1.1\frac{kJ}{g}$ is melting energy, $\vartheta = \mathbf{0.33}$ is Poisson ratio.

The problem geometry is presented in Fig.1. Impact of two aluminum plates at an angle of 14 degrees was simulated. The perturbation of $\lambda_0 = 0.5mm$ wavelength and $a_0 = 0.01mm$ amplitude was given on the surface of the lower rod (Fig.2).

The computational grid is depicted in Fig.3.

Domain 1: impacting plate of 4 mm thickness.

Domain 2: immovable plate of 15 mm thickness, on the external boundary of which initial perturbation $\boldsymbol{a = a_0 \cdot \sin \frac{2\pi}{\lambda_0} x}$ is given.

Domain 3: vacuum.

During the computation the grid remains immovable, fixed. The material moves relative to the immovable computational grid. This allows computations with severe interface strains.

To follow the evolution of the interface between the upper and lower aluminum rods, they were marked with different marks, to be more exact, as “different materials” with identical physical properties. Hence, if material from the upper and lower plates gets into the same computational cell, it is possible to determine the plate interface position by the material concentrations and follow the perturbation evolution.

The computational grid was taken such, that there were on the order of 20 computational cells per wavelength. The total number of the points is 1120x740=828800. The computations in the scalar (one-processor) regime are problematic. So the computations were performed on the shared memory multi-processor computer with complex LEGAK-MP [6].

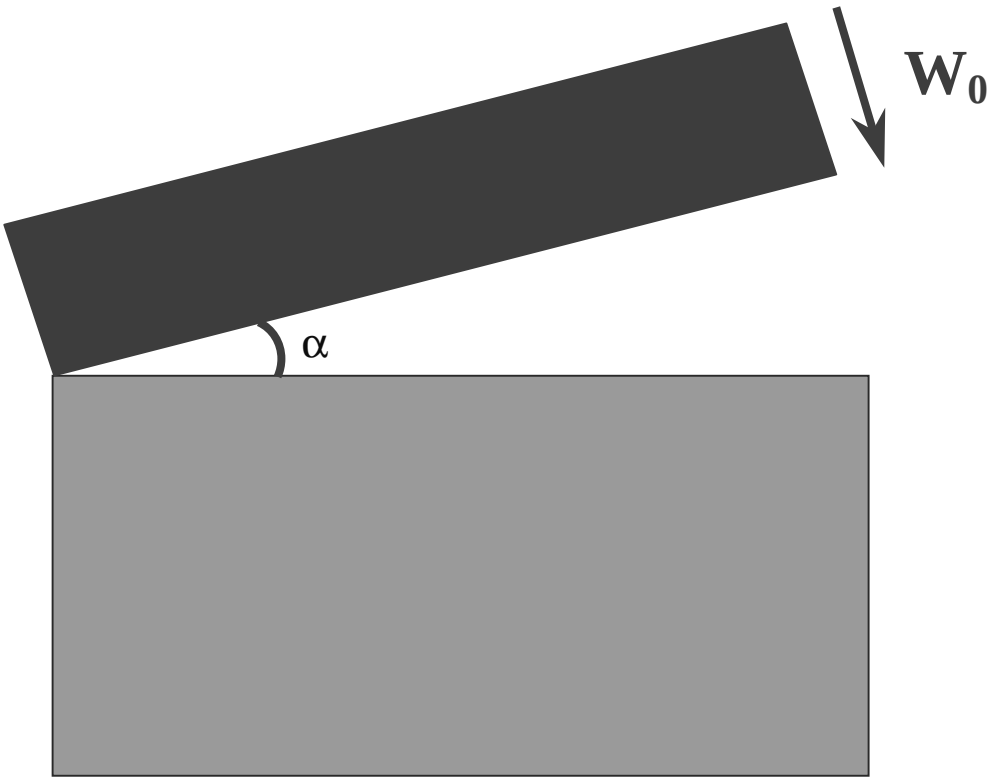

Fig.1 *Problem geometry*

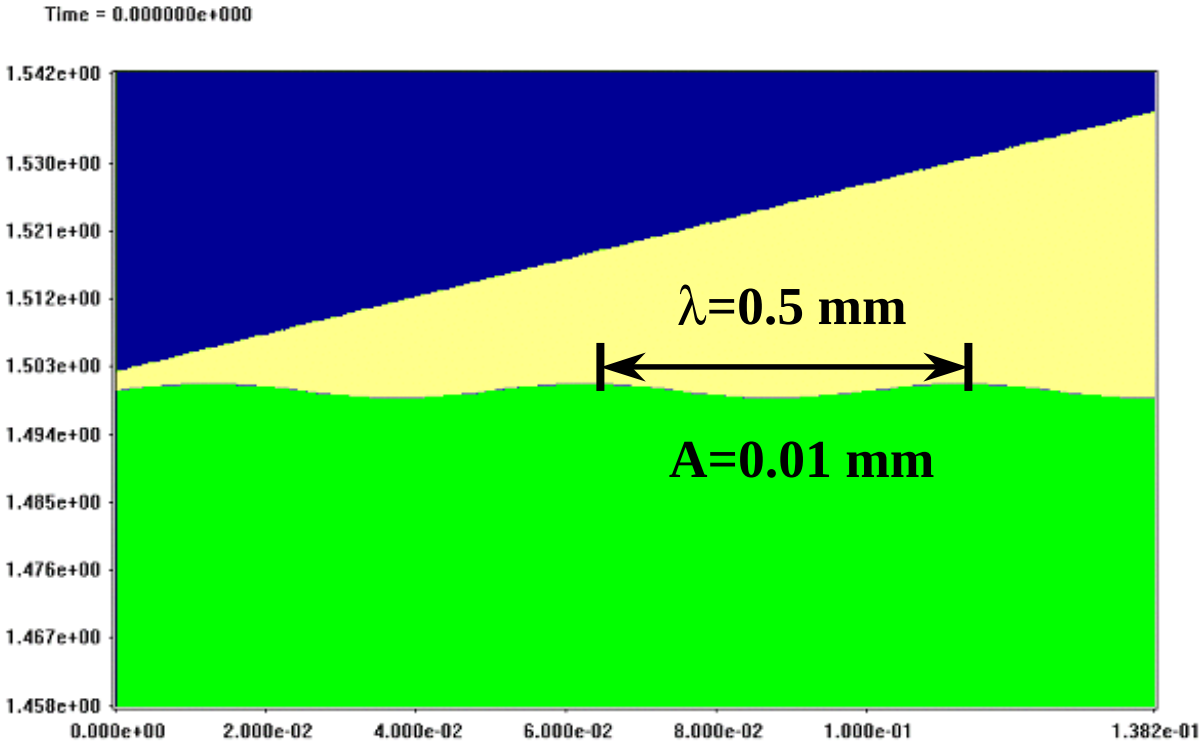

Fig.2 *Initial perturbation*

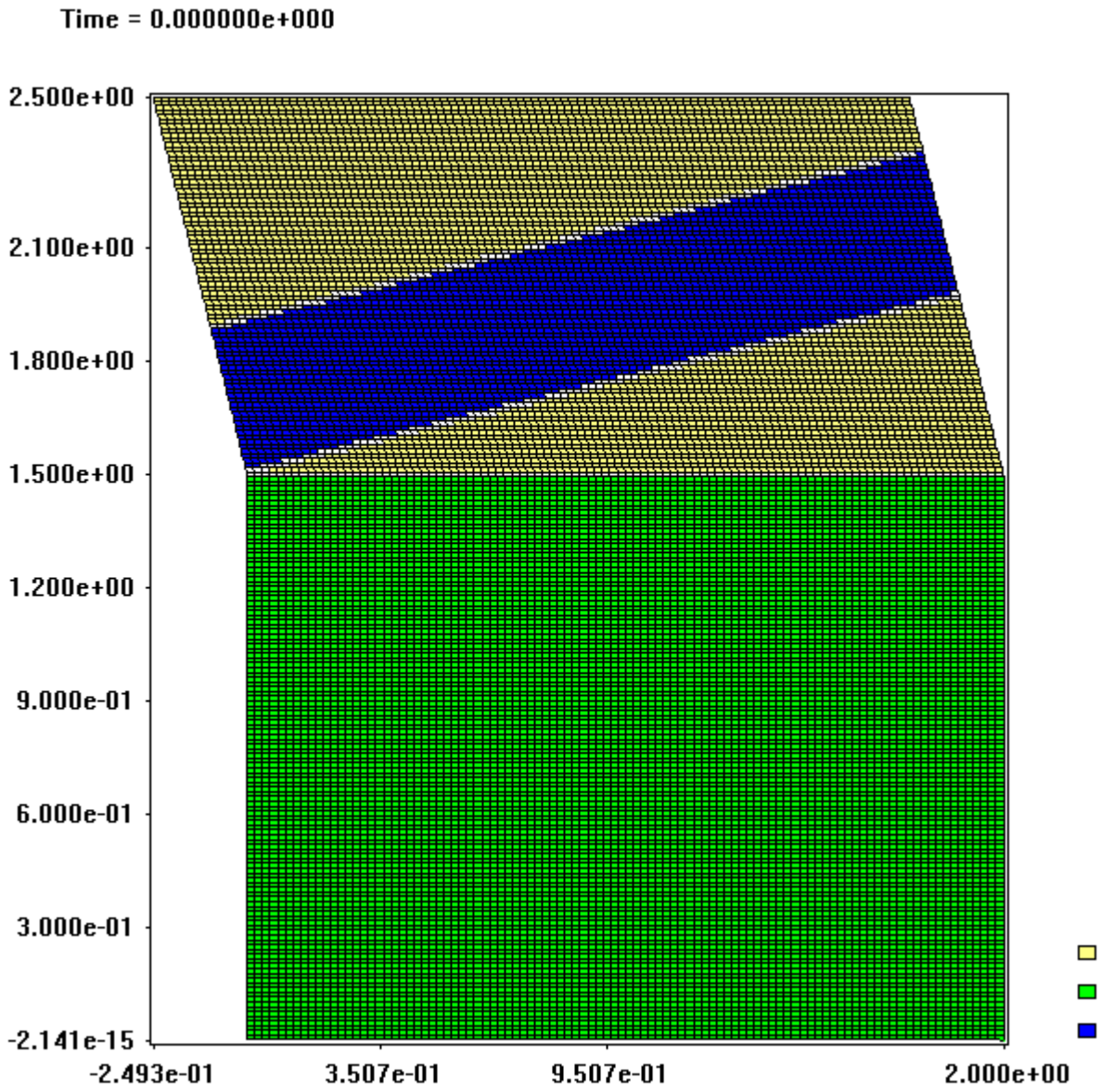

Fig.3 *Computational grid (Eulerian computation)*

At the initial study phase, the computations were performed in the quasi-Lagrangian formulation. In these computations, both the upper (launched) and lower plates were considered as separate regions, whose boundaries were Lagrangian lines, between which there was no interaction. In the areas of the plates, the distances between which became less than ***0.1h*** (where ***h*** is the computational grid size) during the motion, their boundary segments were integrated, thereby the inter-plate interaction was given. A number of computations were conducted in this formulation. The computed data for early times are in a good agreement with the computations on the Eulerian grid. However, because of the grid distortion (due to the complex flow) and other computational "phenomena" it was impossible to perform the computations up to the times of our concern. For this reason our choice was in favor of the computations on the immovable Eulerian computational grid.

2 Results of the computations

Several computational series were conducted. The following was varied in the computations:

- plate impact velocity W_0;
- perturbation wavelength λ_0;
- material properties:
  - gas-dynamic approximation;
  - elastic-plastic approximation with different medium parameters:
    - — variations of strengthening α,
    - — variations of yield strength Y_0,
    - — variations of melting heat E_m,
    - — determination of E_m according to the Lindemann model.

It is of interest to perform the computations including the elastic stress relaxation. This model is being introduced to the program complex LEGAK, and we are planning the studies at the next phase of the work. We are inspired by the fact that the relaxation models most adequately describe material shear strain that is responsible for the perturbation growth in the oblique impact of plates.

2.1 Impact velocity effect

The impact velocity was varied in the computations.
The results for all the computations are presented for the time, when the contact point has traveled a distance of ***L= 20mm***.

The computations were conducted with strengthening factor $\alpha = \frac{1}{3}$, melting heat $E_m = 1.1\frac{kJ}{g}$, and perturbation wavelength $\lambda_0 = 0.5mm$.

The computed amplitude increase factors are summarized in Table 1.

Table 1

Initial velocity W_0, km/s	Amplitude increase factor a/a_0
1.5	6
1.75	2.5
2	1

The perturbation evolution pattern for W_0=1.5 and 1.75 km/s is presented in Figs. 8 and 4.

Thus, the direct numerical simulation reproduces the experimentally detected effect of the perturbation increase.

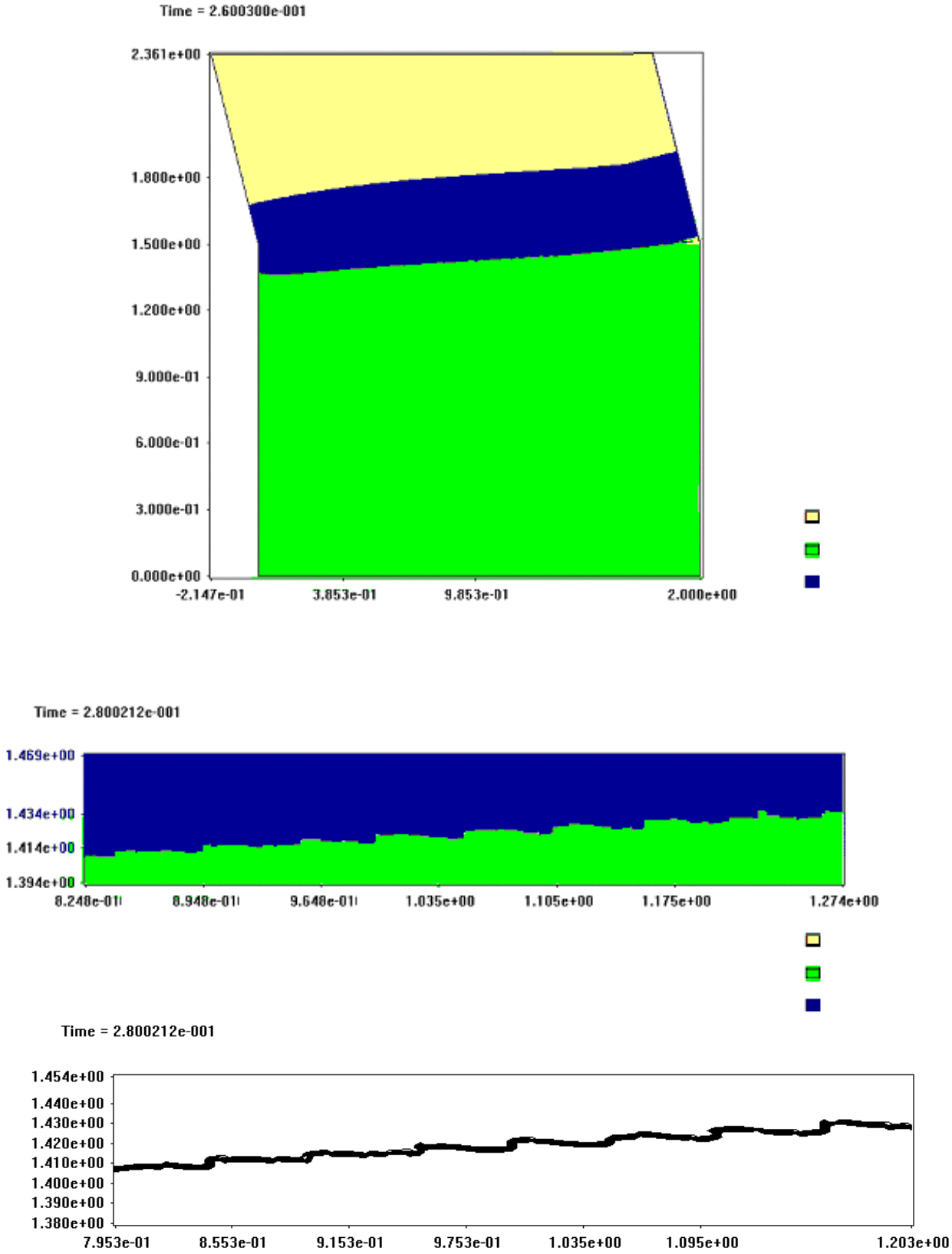

Fig.4 Geometry and isolines (UP $\alpha=1/3$, $U_0=1.75$, $\lambda_0=0.5mm$)

2.2 Simulation of metal interface instability with change in strength properties

The material strength properties were varied in the computations.

The computations were conducted with initial velocity W_0=1.5km/s, melting heat $E_m = 1.1\frac{kJ}{g}$, and perturbation wavelength $\lambda_0 = 0.5mm$.

The perturbation growth pattern is depicted in Figs. 5-8. The material strength effect on the perturbation growth is summarized in Table 2.

Table 2

Material model	Amplitude increase factor a/a_0
Gas dynamics	93
Elasticity-plasticity $\alpha = 0$	65
Elasticity-plasticity $\alpha = 0.1$	53
Elasticity-plasticity $\alpha = 1/3$	6
Elasticity-plasticity $\alpha = 2/3$	2
Elasticity-plasticity $\alpha = 1$	1

2.3 Simulation of metal interface instability with different values of melting heat

The value of melting heat was varied in the computations.

The computations were conducted with initial velocity W_0=1.5km/s, strengthening factor $\alpha = \frac{1}{3}$, and perturbation wavelength $\lambda_0 = 0.5mm$.

The effect of different melting heat values on the perturbaton growth is summarized in Table 3.

Table 3

Melting heat $E_m\left(\frac{кДж}{г}\right)$	Amplitude increase factor a/a_0
0.4	29
1.1	6
1.5	2
2.0	1

2.4 Simulation of metal interface instability with different initial perturbation wavelengths

The computations were conducted in the elastic-plastic approximation ($Y_0 = 0.3$, $\alpha = \frac{1}{3}$, $\beta = 1$) for initial velocity W_0=1.5km/s with different initial perturbation wavelengths.

The results are summarized in Table 4.

Table 4

Initial wavelength (*mm*)	Amplitude increase factor a/a_0
0.25	1
0.5	6
1.0	1

Thus, the ~ 0.5-mm-wavelength perturbations grow most intensively under the discussed conditions. This can explain the fact that among the whole spectrum of the perturbations that take place on “smooth” plates by virtue of their machining it is ~ $0.5 \div 0.6$-mm-wavelength perturbations that grow and are observed in the experiments.

2.5 Change in perturbation wavelength

The computations revealed an interesting fact of increase in the initial perturbation wavelength. The computed data for initial velocity W_0=1.5km/s and wavelength $\lambda_0 = 0.05cm$ are presented in Table 5.

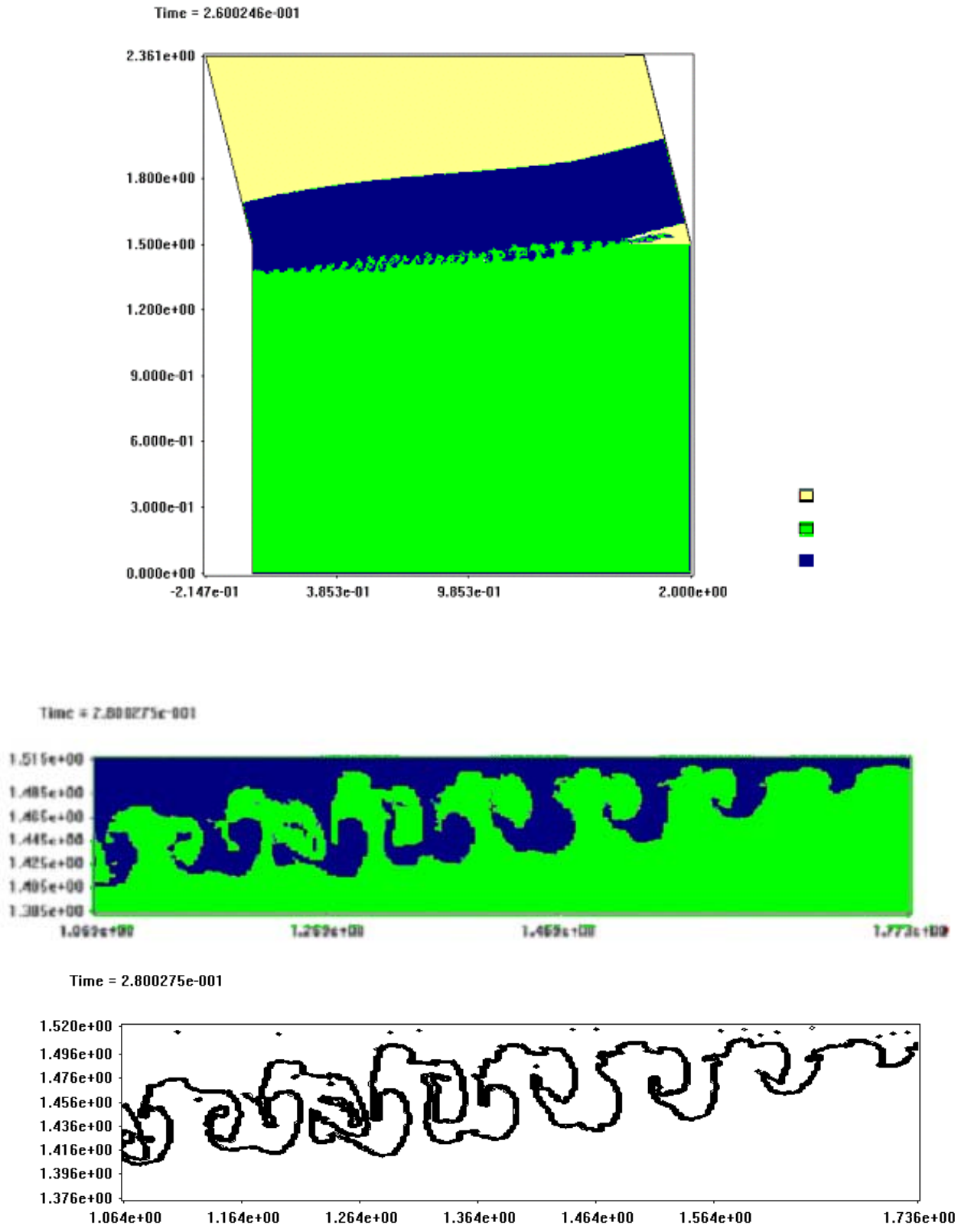

Fig.5 Geometry and isolines (*GD*, U_0*=1.5*, λ_0*=0.5mm)*

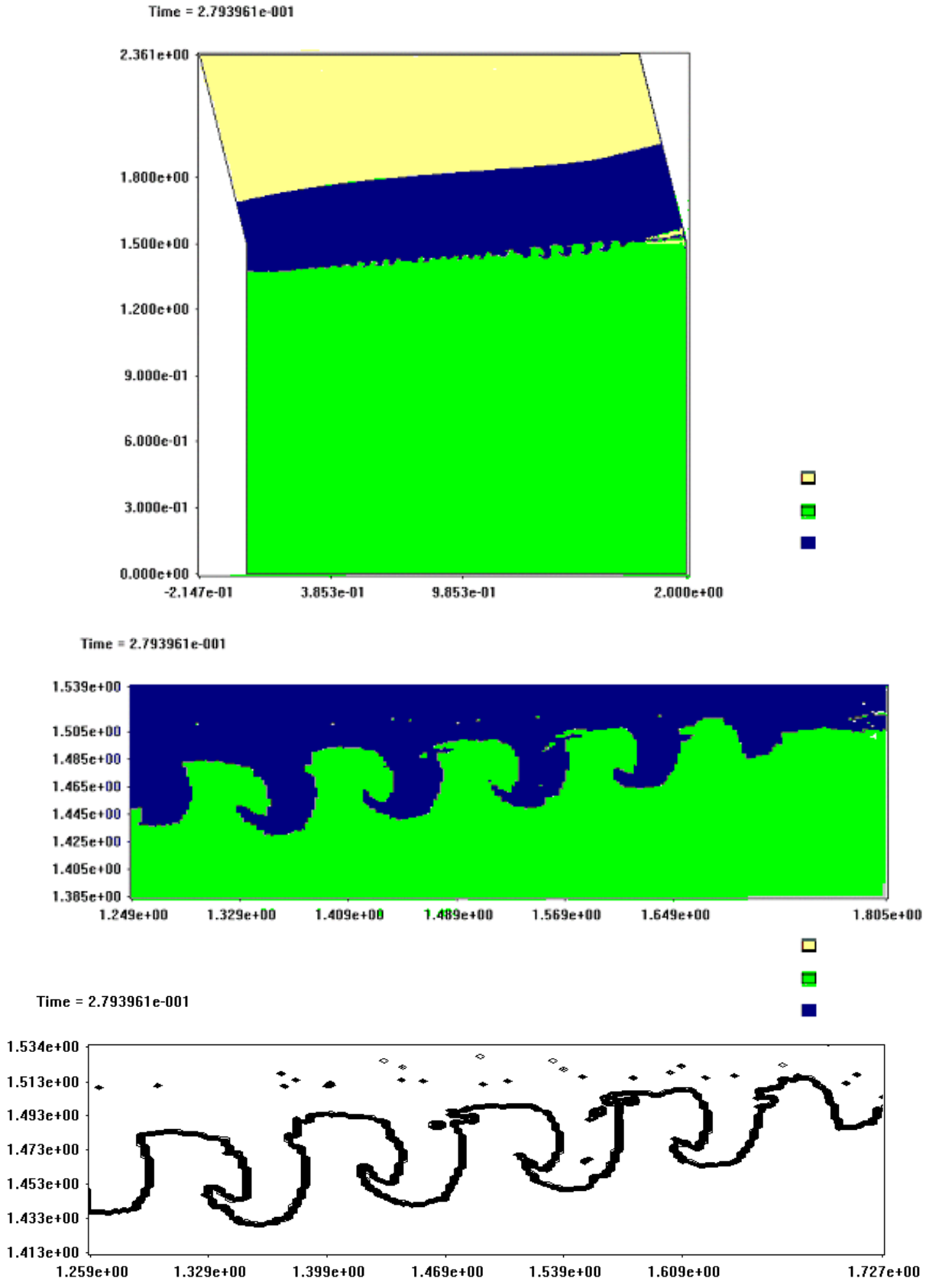

Fig.6 Geometry and isolines (*UP* $\alpha=0$, $U_0=1.5$, $\lambda_0=0.5mm$)

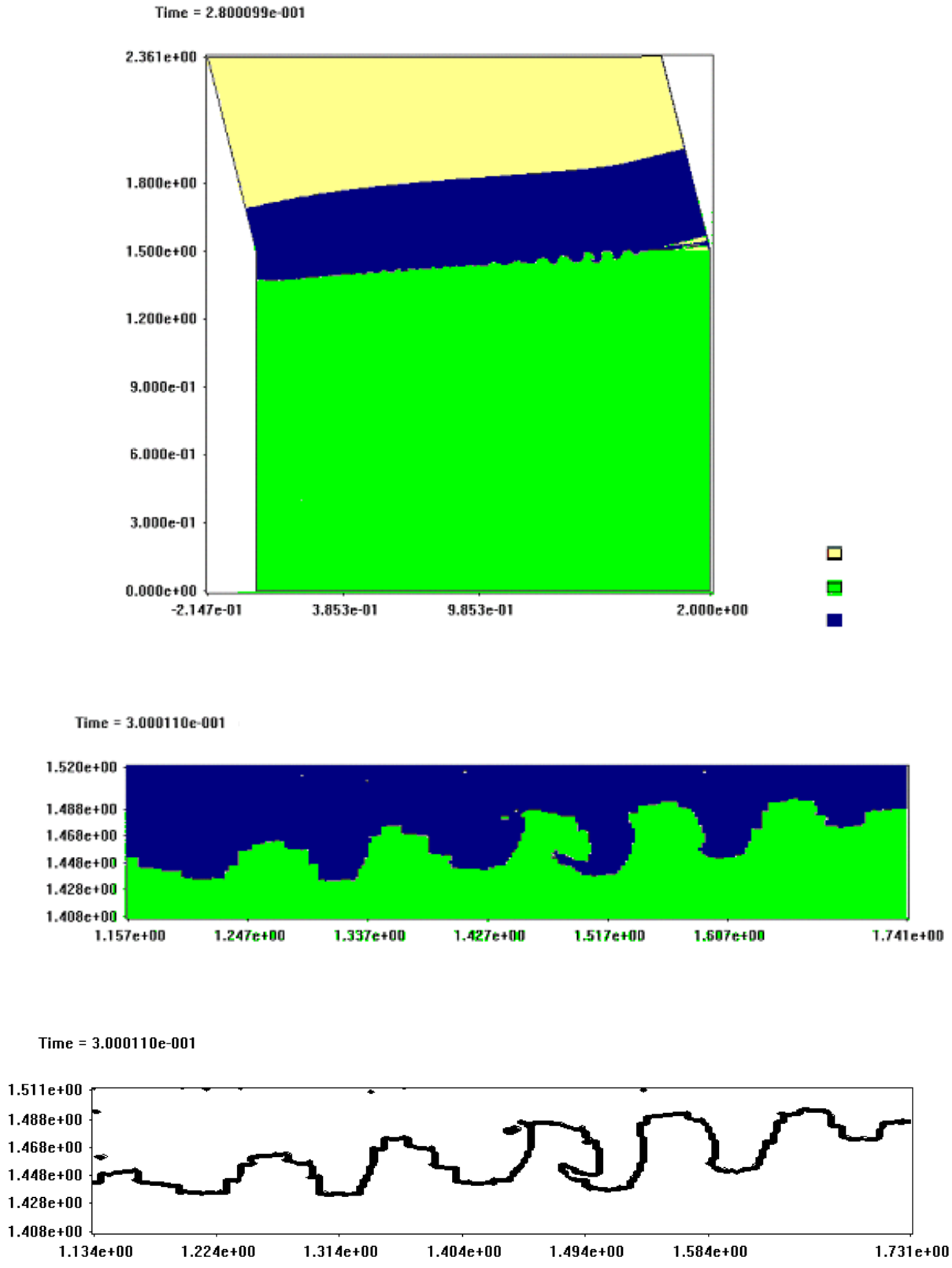

Fig.7 Geometry and isolines (*UP* α*=0.1,* U_0*=1.5,* λ_0*=0.5mm)*

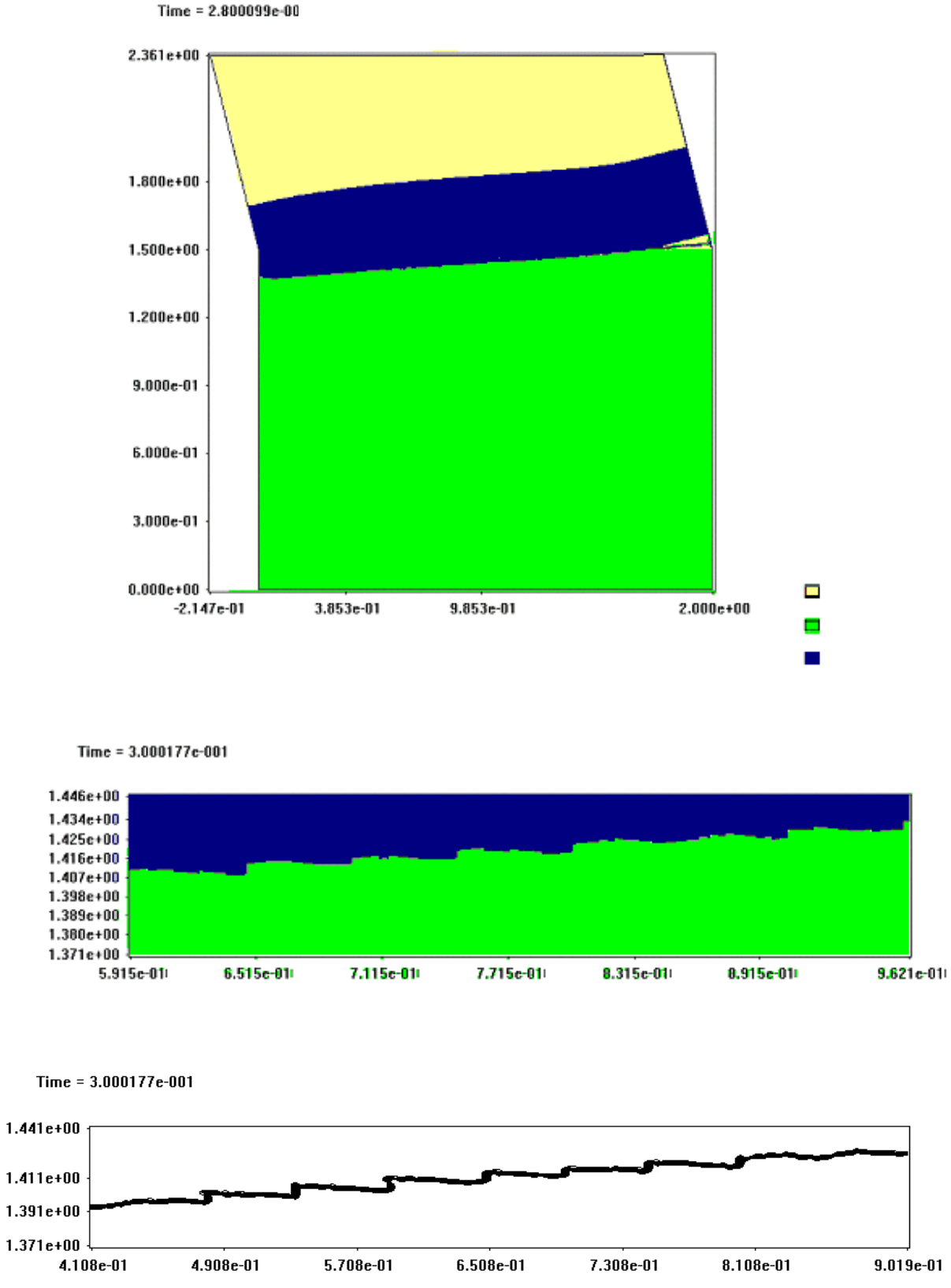

Fig.8 Geometry and isolines (*UP* α*=1/3,* U_0*=1.5,* λ_0*=0.5mm)*

Table 5

Material model	Final wavelength λ *(mm)*
Gas dynamics	1
Elasticity-plasticity $\alpha = \mathbf{0}$	0.9
Elasticity-plasticity $\alpha = \mathbf{0.1}$	0.8
Elasticity-plasticity $\alpha = \mathbf{1/3}$	0.5

Whereas the wavelength increases by a factor of about 2 in the gas-dynamic approximation, it remains essentially unchanged in strong medium. This phenomenon requires more comprehensive study, both numerical and experimental.

Conclusion

The computed data for the oblique plate impact agrees with the experimental data. In particular, it is numerically corroborated that the perturbations of wavelength λ=0.5mm grow most intensively. The numerical simulation revealed the effect of the wavelength growth in low-strength material, which needs more comprehensive study, both experimental and computational.

The work was carried out under the support by Russia Fundamental Research Foundation, Grant 99-01-00812 and 02-01-00796, and LNLN/VNIIEF Agreement B512135.

References

1. Deribas A.A. Strengthening and explosive welding physics. Novosibirsk, Nauka Publishers. 1980.

2. Drennov O.B., Mikhailov A.L., Nizovtsev P.N., Rayevsky V.A. Perturbation evolution at metal interface in oblique impact with contact point moving at supersonic velocity. VANT. Ser. Teoreticheskaya i Prikladnaya Fizika (to be published).

3. Bakhrakh S.M., Spiridonov V.F., Shanin A.A. A method for heterogeneous medium gas-dynamic flow computations in Lagrangian-Eulerian coordinates// DAN SSSR, 1984, V. 278, No. 4, pp. 829-833.

4. Bakhrakh S.M., Kovalev N.P., Pavlusha I.N. A method for elastic-plastic flow computations// Proceedings of All-Union Conference on Numerical Methods of Elasticity and Plasticity Theory. Part I. Novosibirsk, Nauka Publishers. 1974, pp.22-36.

5. Zeldovich Ya.B., Raizer Yu.P. Physics of shock waves and high-temperature hydrodynamic phenomena. Moscow, Fizmatgiz Publishers, 1963, 632p.

6. Avdeyev P.A., Artamonov M.V., Bakhrakh S.M., Velichko S.V., Volodina N.A., Vorobyeva N.M., Yegorshin S.P., Yesayeva E.N., Kovaleva A.D., Luchinin M.V., Pronevich S.N., Spiridonov V.F., Taradai I.Yu., Tarasova A.N., Shuvalova E.V. Program complex LEGAK and principles of its parallelization on multiprocessor computers// VANT. Ser. Matematicheskoye Modelirovaniye Fizicheskikh Protsessov (to be published).